



14<sup>th</sup> IEA Heat Pump Conference  
15-18 May 2023, Chicago, Illinois

# On the Use of CO<sub>2</sub> as a Heat Distribution Fluid for Sustainable Ammonia Heat Pump Solutions

Matt Robinson<sup>a</sup>, Aaron Tam<sup>a</sup>, Scott Goedeke<sup>a</sup>, Dennis Nasuta<sup>b</sup>, Paul Kalinowski<sup>b</sup>,  
and Andrea Mammoli<sup>c</sup>

<sup>a</sup>Electric Power Research Institute, 1001 Data Lane, Knoxville, TN, 37932, USA

<sup>b</sup>Optimized Thermal Systems Inc., 7040 Virginia Manor Rd., Beltsville, MD, 20705, USA

<sup>c</sup>Sandia National Laboratories, 1515 Eubank SE, Albuquerque, NM, 87123, USA

---

## Abstract

Supercritical CO<sub>2</sub> is receiving increased interest as a heat transfer fluid, particularly in heat pump applications, due to some favorable physical properties. While supercritical CO<sub>2</sub> is traditionally circulated via compressors, it may be possible to use centrifugal pumps as an alternative. This could lead to substantial energy and cost savings. The design and evaluation of a pumped supercritical test loop is reported in this work. Upon verifying supercritical CO<sub>2</sub> could be circulated with the pump in the given setup, conditions were varied to understand the behavior of the pump and the potential for acting as a heat transfer loop between an outdoor heat pump and the indoor space. These results are presented along with suggestions for improved performance and problems that were encountered in the work.

© HPC2023.

Selection and/or peer-review under the responsibility of the organizers of the 14<sup>th</sup> IEA Heat Pump Conference 2023.

*Keywords: Pumped Supercritical CO<sub>2</sub>; HVAC; Low GWP*

---

## 1. Introduction

There are two interrelated trends in the power and energy industries to meet climate stabilization goals. The first is the electrification of fossil fuel-based end use technologies and the second is the decarbonization of electricity generation. The technology of choice for electrification of heating is generally the heat pump, which can replace fossil fuel-based furnaces and water heaters. The trend of using heat pumps to replace these technologies is likely to increase with next generation heat pumps capable of handling colder ambient conditions.

While heat pumps offer a route to electrify heating technologies, they rely on refrigerants that can have orders of magnitude larger global warming potential (GWP) than CO<sub>2</sub>. With this, the Heating, Ventilation, and Air Conditioning (HVAC) industry is experiencing a push to low GWP refrigerants. The American Innovation and Manufacturing (AIM) Act has directed the Environmental Protection Agency (EPA) to *phase down production and consumption of hydrofluorocarbons* (HFCs), due to their high global warming potentials (GWPs) [1]. This planned reduction in production and consumption, while not directed at air conditioners and heat pump systems is consistent with the transition towards more environmentally friendly refrigerants. From a system designer and manufacturer perspective, what options are available? There is a large interest in natural refrigerants such as ammonia (R-717), CO<sub>2</sub> (R-744), and propane (R-290) which are low GWP but *tend* to be more toxic and/or flammable. The synthetic refrigerant alternatives such as R-32 and R-454B have lower GWPs but are still orders of magnitude greater than that of the mentioned natural refrigerants and are more costly. Given the trend towards lower GWPs, facility and plant managers in commercial buildings, and industrial and commercial refrigeration may be faced with decisions of cost and compliance (if it comes to that point) on which systems to utilize to meet their building cooling and heating and/or their refrigeration needs.

Previous research done at the Electric Power Research Institute (EPRI) investigated technologies that can provide solutions/options for low GWP heating and cooling. EPRI performed a laboratory evaluation of a 35

kW (10 RT) ammonia chiller that used CO<sub>2</sub> as the heat transfer fluid to the indoor units [2]. Ammonia was selected as the refrigerant due to its performance and low GWP. The major drawback of this selection is the toxicity of ammonia which requires the ammonia side of the system to be contained outside, requiring a secondary heat transfer loop. Typically, a water-glycol mixture would be used as the working fluid in the secondary loop, however, the work showed the benefits of using liquid CO<sub>2</sub> as the working fluid between the indoor and outdoor units. The main advantage was due to the large latent heat of vaporization of CO<sub>2</sub>, taking advantage of phase changes. This resulted in the ability to use smaller diameter pipe and low mass flow rate to transfer heat between indoor air handling units (AHUs) and the ammonia chiller.

This paper presents a novel concept of utilizing a CO<sub>2</sub> secondary loop for space cooling *and* heating with an ammonia based outdoor unit. Specifically, the ability of a CO<sub>2</sub> pump to circulate supercritical CO<sub>2</sub> is investigated, because the critical temperature of CO<sub>2</sub> (304.25 K) is lower than the temperature typically delivered to heating coils (assuming the volume is such that the pressure is beyond the critical pressure; a likely scenario in HVAC applications).

Centrifugal pumps and compressors both move fluid by accelerating it through vanes in a spinning impeller and then increasing the pressure at the outlet by converting part of the kinetic energy imparted. In a pump the fluid is usually a liquid whose density remains approximately constant, while in a compressor the working fluid is a gas whose density is increased. There are substantial differences between impeller designs in centrifugal compressors and pumps. For supercritical CO<sub>2</sub> applications near the critical point, the working fluid is closer to a liquid than to a gas. Nevertheless, the geometry for optimal pumping of supercritical CO<sub>2</sub> is not the same as for an incompressible fluid, and it is a function of the thermophysical properties of the CO<sub>2</sub>. A number of studies investigated these issues in connection with applications in oil and gas, and in power generation. Through a CFD analysis, Cubas et al. [3] conclude that typical hydrodynamics similarity laws of pumps used with liquids can be used to evaluate performance when pumping a supercritical fluid. Kim et al. [4] compare experimental and numerical results and conclude that CFD can yield insight into the performance of liquid pumps used for supercritical CO<sub>2</sub>, and moreover that liquid pumps can pump supercritical CO<sub>2</sub> effectively. Bergamini et al. [5] provide similar conclusions, namely that centrifugal pumps are efficient means of pumping supercritical CO<sub>2</sub>, provided that certain conditions of temperature and pressure are met. While the pump used in this application is much smaller than what would be considered for oil recovery, CO<sub>2</sub> sequestration, or power generation, we too expect the performance in pumping supercritical CO<sub>2</sub> to be similar to the rated performance of the pump for liquid CO<sub>2</sub> applications.

There are numerous benefits of pumping supercritical CO<sub>2</sub> for the current ASHP design, mainly because a CO<sub>2</sub> compressor will not be required. The pumped solution offers lower electrical power consumption, reduces the total cost of the system, and provides a simpler overall design.

This paper presents the testing of a CO<sub>2</sub> pump to circulate supercritical CO<sub>2</sub> in EPRI's Knoxville Thermal Laboratory. The following sections describe the setup that was used to test the idea, the results from the tests that were performed, and a discussion on areas for improvement and further study for this application.

## 2. Experimental Setup

The experimental setup was designed to mirror the conditions that the supercritical CO<sub>2</sub> would experience in the secondary loop that transfers heat from the condenser to heating coils inside a building. In particular, a test loop was constructed to mimic the heating mode of an ASHP that is connected to the indoor space by a CO<sub>2</sub> loop. The CO<sub>2</sub> is pumped into the condenser of the ASHP where it is heated, routed to the indoor AHUs where it heats the air and then pumped back to the condenser of the ASHP. The test loop is a scaled version of this loop. Heat exchangers (HXs) are paired with valves to simulate behavior of the real heat exchangers, namely heat transfer with pressure drops. The layout of the test loop is explained in detail below.

## 2.1. Test loop hardware details

The test loop is composed of the CO<sub>2</sub> pump, two compact plate HXs, needle valves to provide controlled pressure drops, a receiver to act as a buffer for the pump, measurement devices (flow meter, digital pressure transducers, analog pressure transducers, and thermocouples), and valves for charging, venting, and vacuuming the system. A schematic of the system is shown in Figure 1 and a part list is presented in **Error! Reference source not found.** The CO<sub>2</sub> pump is a dual stage centrifugal pump where the impellers are magnetically coupled to the motor. The pump was selected because it is designed to pump liquid CO<sub>2</sub> and is rated for

Table 1: Primary components in test loop.

Component	Manufacturer	Part Number	Notes
CO <sub>2</sub> Pump	Hy-Save	820-DS-050-VSD-B	12 MPa Max
Brazed Plate Heat Exchanger	SWEP	B4TMx30	14 MPa Max
Coriolis Flow Meter	Emerson	CMFS025MB67N2BAEKZZ	10.3 MPa Max
Needle Valves	Swagelok	SS-18RS8	> 20 MPa
Digital Pressure Sensor	ProSense	SPT25-10-2000A	0-13.8 MPa F.S.
Cu-Fe Tubing	Mueller Streamline	N/A	13 MPa rating

pressures suitable for handling supercritical CO<sub>2</sub>. The tubing connecting the components is copper-iron (Cu-Fe) tube rated for 13 MPa and can be brazed using standard equipment and a high silver content braze rod. The fluid is first circulated through a MicroMotion Coriolis flow meter rated at 10.3 MPa which measures the

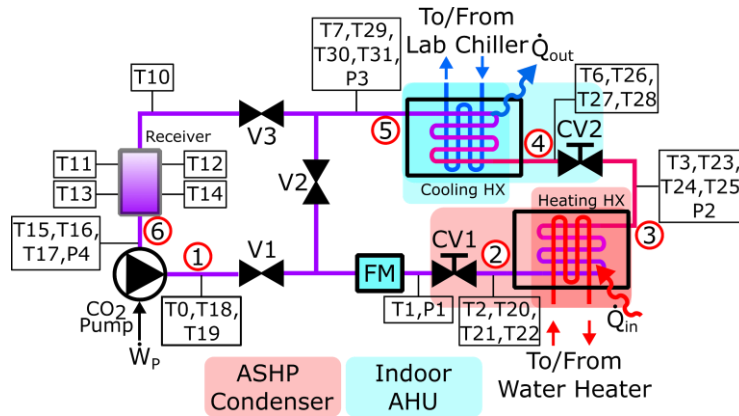


Figure 1: Schematic of test loop for evaluating supercritical CO<sub>2</sub> pumping. T and P indicate location of temperature and pressure measurements, respectively. CV1 and the heating heat exchanger act as the heating portion of the ASHP while CV2 and the cooling heat exchanger act as the indoor air handling unit (AHU).

flow rate and the density of the fluid. The fluid then goes into the part of the loop acting as the condenser of the ASHP. First the fluid passes through a stainless-steel needle valve to simulate pressure drop along the heat exchanger. The CO<sub>2</sub> is then heated in a brazed plate heat exchanger (BPHE) referred to as the heating HX. The heating HX's heat source is 0.15 m<sup>3</sup> (40 gallon) electric water heater coupled with a small circulating pump. The heated CO<sub>2</sub> then passes through the section of the test loop acting as the indoor AHU. The CO<sub>2</sub> passes through another needle valve, providing a controllable pressure drop, and is then cooled by another BPHE, referred to as the cooling HX. The cooling fluid is provided by a water loop in the laboratory, which is cooled by a chiller and heated by electric heaters, following a given setpoint. After the CO<sub>2</sub> is cooled it is collected in a receiver. The receiver has two functions. First it adds additional volume for a fluid reservoir to be available for the pump, ensuring that the pump doesn't run out of fluid to pump. Secondly, the receiver helps ensure that the pressure head requirement for the pump is met. The amount of pressure drop between the receiver and the inlet of the pump is also minimized per the manufacturer recommendation. The CO<sub>2</sub> pump operates on 208 VAC three-phase and a variable speed drive (VSD) is used to control the speed. A bypass was added to the loop in the scenario when not enough fluid is being returned to the pump to cool the motor. This condition has

not been observed with the testing so far. A pressure relief valve was added to protect components and safely reduce the pressure, if exceeded. The system was pressure tested and the pressure relief valve set to 9.75 MPa (1,414 psia). Considerations must be taken with the pressure relief valve if it were ever to exhaust. High pressure CO<sub>2</sub> when rapidly expanded can cause dry ice to form, potentially blocking the exhaust path. Because of this, connecting tubing on the exhaust of a pressure relief valve with CO<sub>2</sub> systems should be avoided. Instead, the CO<sub>2</sub> is allowed to exhaust into the laboratory space where CO<sub>2</sub> sensors are integrated with exhaust fans.

Figure 1 also indicates the measurements being taken and their locations. Temperature is measured using T-type thermocouples and two NI USB-9213 thermocouple modules. 32 temperature measurements are monitored with important measurements (in and out of the heat exchanger, for example) being made with multiple thermocouples. The thermocouples are taped to the pipe and the piping is insulated. The thermocouples were calibrated in a temperature bath prior to installation into the system. Pressure is measured by digital and analog pressure gauges. The four digital sensors output a 0-10 VDC which is read by an NI USB-6001. The flow meter and power meter provide a Modbus over RS-485 interface that the data acquisition computer queries for measured values. Figure 2 shows the completed test setup with major components identified.

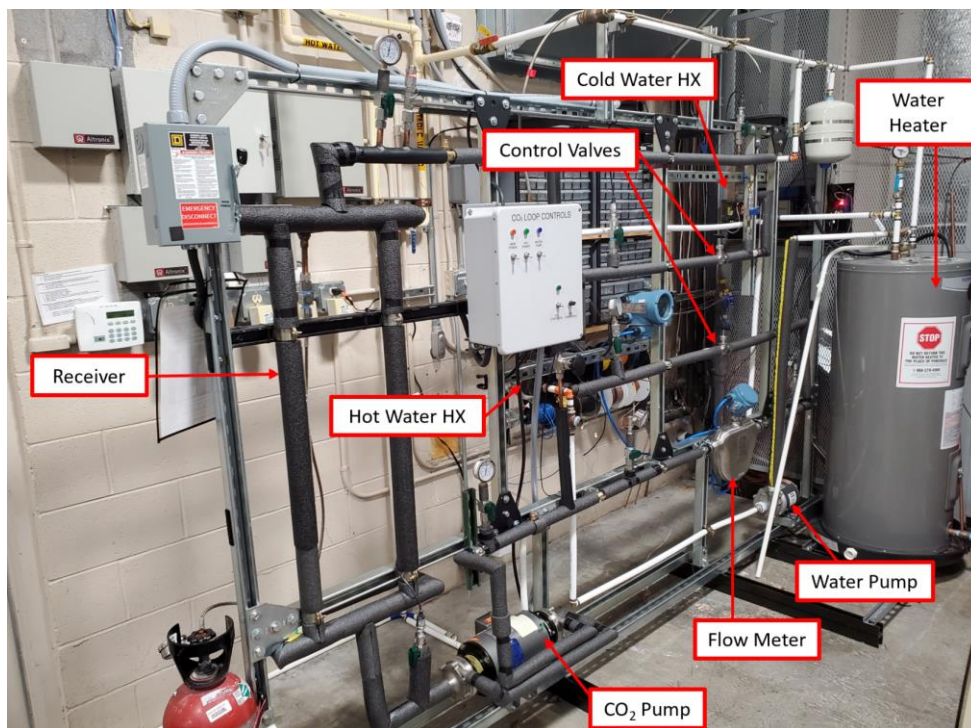


Figure 2: The supercritical CO<sub>2</sub> pump test loop as-built. The insulated lines are the CuFe tubes that contain the CO<sub>2</sub>. The water lines, hot and cold, are plumbed in PEX (white pipes in figure).

## 2.2. Charging of the test loop

The mass of CO<sub>2</sub> to be added to the system (commonly called the charge) was based on the density of supercritical CO<sub>2</sub> at 309 K and 8.5 MPa, and an estimate of the volume of the system. The particular value chosen is a compromise between maximizing the specific heat,  $c_p$ , and the stability of  $c_p$  at the particular fluid

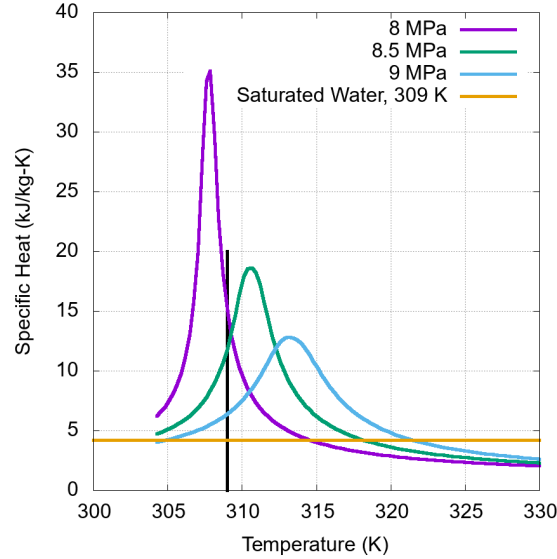


Figure 3: The specific heat of supercritical CO<sub>2</sub> as a function of temperature and pressure. The black vertical line indicates the design temperature for the indoor AHUs.

conditions. Figure 3 illustrates this tradeoff as  $c_p$  of supercritical CO<sub>2</sub> is plotted as a function of temperature for different pressures with the black vertical line showing the desired temperature of the fluid going into the indoor AHUs (design condition). As the pressure increases the specific heat decreases but the curves also flatten out, making  $c_p$  more stable. It was decided that if we could operate around the 8.5 MPa curve, that would be a reasonable balance between stability and large  $c_p$ . For reference,  $c_p$  of saturated liquid water at 309 K (4.2 kJ/kg-K) is also shown on Figure 3. The mass required is given by,

$$m = \rho V \quad (1)$$

where  $\rho$  is the density at the design condition and  $V$  is the volume of the system. The system volume is estimated to be 3.4E-3 m<sup>3</sup> and the density is 568 kg/m<sup>3</sup> at the design condition. The required mass to be fill the system is 1.9 kg. The actual charge of the system was 2.2 kg to provide a slight additional charge for the system in-case of uncertainties in volume estimates. The filling process begins with pulling a vacuum on the system. When the vacuum is sufficient, a CO<sub>2</sub> cylinder with a dip tube is placed on a scale and connected to the fill valve and liquid CO<sub>2</sub> is pulled from the bottom of the cylinder. CO<sub>2</sub> is pressure fed into the system until the correct mass has been reached. If the pressure between the system and the cylinder balances before the required mass is in the loop, heat can be applied to the cylinder to increase the pressure in the cylinder, thereby pushing more liquid CO<sub>2</sub> into the loop.

## 3. Test Method

The primary goal of testing was to see if it would be possible to pump supercritical CO<sub>2</sub> effectively using a pump designed for liquid CO<sub>2</sub>. If pumping was possible, a series of tests would be conducted to examine the performance of the pump over a range of conditions. In particular the following are held constant over the course of a test:

- Temperature entering pump
- Temperature exiting heating HX
- VFD frequency
- Position of CV1 and CV2



The temperatures in the first two bullets were held constant by adjusting valves on the water side of the associated heat exchangers. The frequency of the VFD was set on the drive's front display and the control valves were set before the start of a test. To get the test loop to test conditions (supercritical CO<sub>2</sub> flowing) the cooling water loop and heating water loop were operated until steady state was reached for their control setpoint. The CO<sub>2</sub> pump was started at about 10 Hz with the cooling water valve closed and the heating water valve about a quarter turn open. The temperature and pressure begin to rise in the system until the CO<sub>2</sub> pressure and temperature go beyond the critical point. At this point, the VFD is adjusted to the test's frequency and the cooling water valve is partially opened. The cooling and heating valves are adjusted until the temperature setpoints for the test are met. The test condition is ran for at least 15 minutes while at steady state.

Referring to Figure 1 (numbers in red circles) the rate of heat added to the system,  $\dot{Q}_{in}$ , can be calculated by

$$\dot{Q}_{in} = \dot{m}(h_3 - h_2) \quad (2)$$

where  $\dot{m}$  is the mass flow rate measured by the flow meter,  $h_3$  is the specific enthalpy of the CO<sub>2</sub> leaving the heating HX, and  $h_2$  is the specific enthalpy entering the heating HX. The specific enthalpy is determined using REFPROP [6, 7] and the measured temperature and pressure at the location. The rate of heat leaving the system through the cooling HX,  $\dot{Q}_{out}$ , is given by

$$\dot{Q}_{out} = \dot{m}(h_5 - h_4) \quad (3)$$

where the  $h_5$  and  $h_4$  refer to the specific enthalpy leaving and entering the cooling HX, respectively. The rate of work on the fluid performed by the pump,  $\dot{W}_p$ , is determined by

$$\dot{W}_p = \dot{m}(h_1 - h_6) \quad (4)$$

where the specific enthalpy is calculated at the outlet of the pump, location 6, and at the inlet of the pump, location 1. The electrical power consumption of the pump,  $\dot{P}_p$ , is calculated assuming a balanced three phase load,

$$\dot{P}_p = \sqrt{3}VIp f \quad (5)$$

where  $V$  is the applied voltage, 208 VAC,  $I$  is the measured current, and  $pf$  is the nominal power factor of the pump, 0.67. The work done by the pump and the amount of electrical power are related through the efficiency,

$$\eta = \frac{\dot{W}_p}{\dot{P}_p} \quad (6)$$

which has a nominal value of 72.5%. Heat engine sign convention is used in this study where heat into and work out of the system are considered positive. At steady state, by the First Law of Thermodynamics,

$$\dot{Q}_{in} + \dot{W}_p = \dot{Q}_{in} + \eta\dot{P}_p = \dot{Q}_{out} + \dot{Q}_{lost} \quad (7)$$

where  $\dot{Q}_{lost}$  is the rate at which heat is lost to the environment.

### 3.1. Uncertainty analysis

Error propagation due to uncertainty in measurements begins with examining Eqns. 2 and 3. In particular, there is a *difference* in enthalpy which is then *multiplied* by the mass flow rate. If uncertainties are independent and random, the uncertainties associated with addition and subtraction is given by [8],

$$\delta\Delta h_{3-2} = \sqrt{\delta h_3^2 + \delta h_2^2} \quad (8)$$

where  $\delta\Delta h_{3-2}$  is the uncertainty that results from taking the difference in enthalpy between points 3 and 2.  $\delta h_3$  and  $\delta h_2$  are the uncertainties associated with the enthalpies. These uncertainties are determined by passing through the uncertainties in the thermocouples and the pressure sensors into the enthalpy calculation

performed by REFPROP. In particular, an upper,  $h_u$ , and lower,  $h_l$ , estimate is made of the enthalpy from the upper and lower bounds of the temperature and pressure. The uncertainty is then determined by

$$\delta h = (h_u - h_l)/2. \quad (9)$$

Given a temperature measurement with associated uncertainty,  $T = T_{best} \pm \delta T$ , and a pressure measurement,  $P = P_{best} \pm \delta P$ ,  $h_u$ , and  $h_l$  are determined by examining the pressure-enthalpy diagram which shows that the upper value of the enthalpy is given by,

$$h_u = f(T + \delta T, p - \delta p) \quad (10)$$

and the lower bound of the enthalpy given the uncertainties in temperature and pressure is,

$$h_l = f(T - \delta T, p + \delta p) \quad (11)$$

where  $f$  is the function for enthalpy provided by REFPROP. It should be noted that this is the worst-case scenario and may be overly conservative. From calibration, a fractional uncertainty of 0.0028 was determined and is assumed for all thermocouples [9]. The pressure sensors have a stated uncertainty of 0.07 MPa. The Coriolis flow meter has a percent uncertainty of 0.25% (assumed for our supercritical case) and a density uncertainty of 0.2 kg/m<sup>3</sup> for *liquids*.

The next consideration is which temperature is used for enthalpy calculations. Multiple measurements of temperature are done at each location, so an average is used. The uncertainty from each measurement is added in quadrature (Eqn. 8) and scaled by  $1/N$  where  $N$  is the number of measurements in the average. For example, the uncertainty of the average of three thermocouples is,  $\delta T_{avg}$ ,

$$\delta T_{avg} = \frac{1}{N} \sqrt{\delta T_1^2 + \delta T_2^2 + \delta T_3^2} \quad (12)$$

where  $\delta T_1$ ,  $\delta T_2$ , and  $\delta T_3$  are the associated uncertainties with thermocouples 1, 2, and 3, respectively, and  $N$  is 3. The relationship between fractional uncertainty,  $x_{frac}$ , and uncertainty,  $\delta x$ , is

$$x_{frac} = \frac{\delta x}{|x_{best}|} \quad (13)$$

where  $x_{best}$  is the measurement made. Using Eqn. 13, Eqn. 12, with constant fractional uncertainty, can be rewritten as,

$$\delta T_{avg} = \frac{T_{frac}}{N} \sqrt{T_{best,1}^2 + T_{best,2}^2 + T_{best,3}^2}. \quad (14)$$

The final uncertainty consideration is how the error from the mass flow meter and the difference in enthalpy combine. This is straightforward because the fractional uncertainty of products and quotients, is the square root of the sum of the squares of the given fractional uncertainties [8].

#### 4. Results

The first test was to verify that the test loop could circulate supercritical CO<sub>2</sub>. Initially the CO<sub>2</sub> is two phase mixture at room temperature. The VFD was operated at a low frequency to circulate the liquid CO<sub>2</sub> while adding heat, to ensure uniformity while avoiding excessive stress on the pump produced by circulating two-

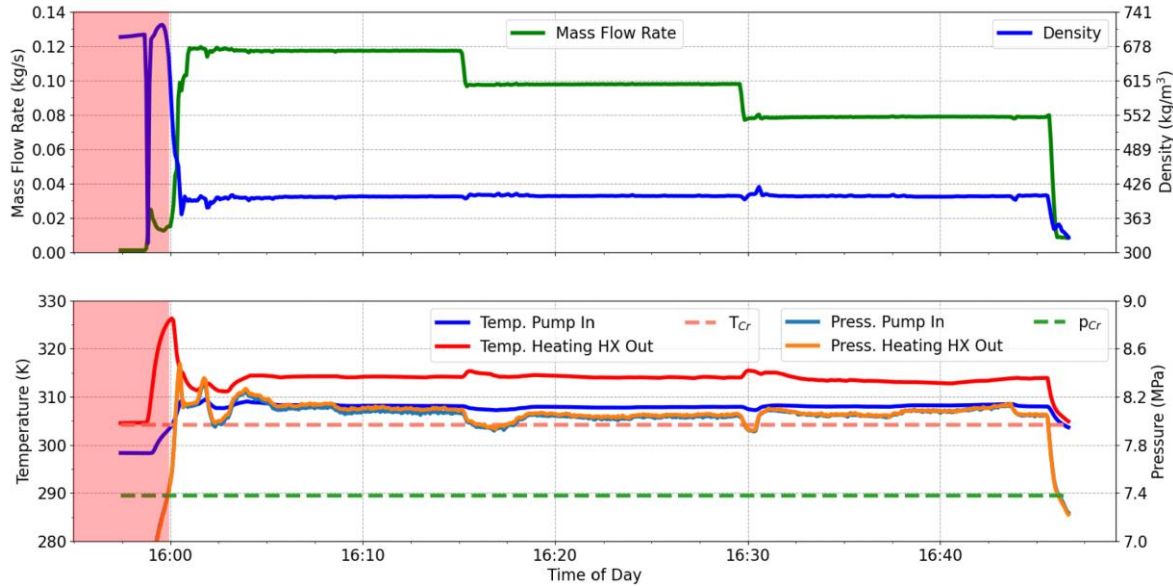


Figure 4: An example of a test performed with a pump inlet temperature of 308.15 K and heating heat exchanger outlet set to 313.71 K. CO<sub>2</sub> goes supercritical after the red transparent rectangles when the temperature and pressure pass their respective critical point values,  $T_{Cr}$  and  $p_{Cr}$ .

phase fluid. The temperature and pressure increased while the density decreased. When enough heat was added the temperature and pressure surpassed the respective critical points. At this point the density stabilized and the VFD frequency was increased. This showed that the pump could circulate supercritical CO<sub>2</sub> and testing could continue, studying how the pump performed in different conditions.

Figure 4 is an example of a test performed with the pump inlet temperature set to 308.15 K and the heating HX outlet temperature set to 313.71 K. Initially the CO<sub>2</sub> is subcritical as indicated by the shaded red rectangles. As heat is added through the heating HX the temperature and pressure increase until the critical point is passed. At this point the cooling heat exchanger valve is opened to stabilize the temperature and pressure. The VFD is set to the frequency for the specific test. The valves on the heating and cooling water are adjusted such that the test conditions are met; temperature setpoints for pump inlet temperature and heating heat exchanger outlet. The pump inlet and heating HX outlet temperatures are monitored during the test period and adjusted. This was more difficult on the heating water loop due to the smaller capacity of the hot water tank. After about 15 minutes of steady-state operation the VFD is then adjusted to the next speed (60 Hz, 50 Hz, and 40 Hz), the valves adjusted for temperature setpoint, followed by another 15-minute period for steady state conditions. The VFD adjustment is seen in Figure 4 with the decreasing steps in the mass flow rate. As the temperature



setpoints were varied the density changed slightly between tests which yielded insight into how the CO<sub>2</sub> pump performed with a varying fluid density, although the changes were minor. **Error! Reference source not found.** illustrates the performance of the pump as the density changes (slightly) and as the VFD frequency is

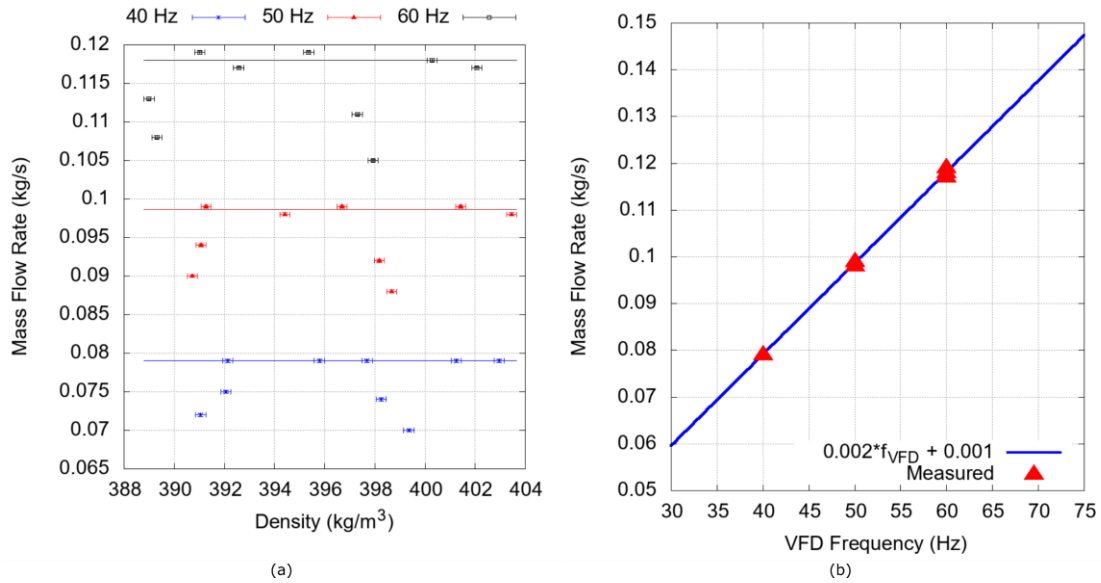


Figure 5: (a) The change in mass flow rate as a function density, VFD frequency, and pressure drop. The blue, red, and black lines represent the average flow rates at 40, 50, and 60 Hz. Large deviations from this average are caused by increased pressure drops due to closing needle valves. (b) The mass flow rate as function of the VFD frequency.

adjusted. For reference, liquid CO<sub>2</sub> at 20 °C has a density around 773 kg/m³. This performance shows that the mass flow rate is a strong function of the VFD frequency, as expected, and does not vary significantly with the variation in density experienced during these tests. The nominal volume flow rate for this pump when used for liquid CO<sub>2</sub>, at 60 Hz, is between 12.1 and 20.8 liters/minute for 19.8 to 13.7 m of head, respectively. The maximum volume flow rate for supercritical CO<sub>2</sub> at the same pump speed was approximately 17.8 liters/minute, confirming expectations that the pumping of supercritical CO<sub>2</sub> would be similar to that of liquid CO<sub>2</sub>. **Error! Reference source not found.** also shows the effect of increasing the pressure drop through the

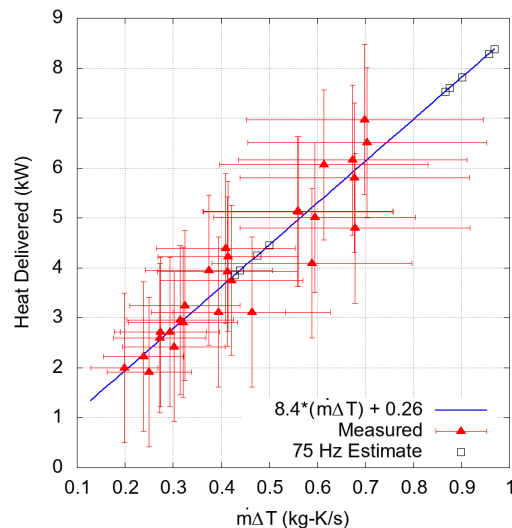


Figure 6: The rate of heat delivered to the cooling heat exchanger as the product of the mass flow rate and change in temperature is varied.

test loop by closing the needle valves a given amount. The blue, red, and black horizontal lines are the average mass flow rates with the needle valves fully open, for 40, 50, and 60 Hz, respectively. Both the heating and

cooling HX valves are closed in equal amounts; first 2 turns and then 3 turns. The decrease in flow rate is seen, again, as expected, by the four points that are away from the averages.

The ultimate purpose of the pump is to deliver heat between the indoor AHU and the ASHP. Figure 6 shows the amount of heat that the pump was delivered as a function of the product of the mass flow rate and temperature difference between the heating HX output and the pump inlet temperature. The rate of heat delivered behaves as expected, increasing as the mass flow rate and/or temperature difference increases.

## 5. Discussion

The presented results show that circulation of supercritical CO<sub>2</sub> is possible with an appropriately pressure rated/designed CO<sub>2</sub> pump. The mass flow rate varied between 0.07 kg/s at 40 Hz to about 0.12 kg/s at 60 Hz. The electric power provided to the pump for these flow rates is between 150 W and 200 W. The alternative to using the CO<sub>2</sub> pump is a CO<sub>2</sub> compressor. The compressor selected for the current project is estimated to draw

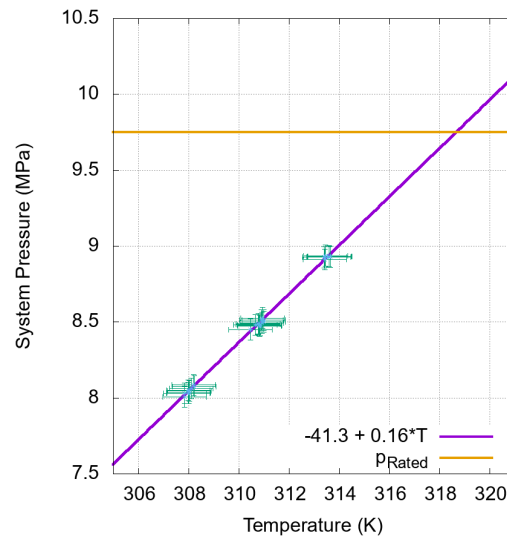


Figure 7: System pressure as function of the pump inlet temperature. The pump inlet temperature should be kept below 319 K to keep the system below the pressure rating.

about 6.5 kW to operate, running at part load. This is a significant difference between using the pump and compressor. The designed heating load is between 35.2 and 70.3 kW which, by inspection of Figure 6, indicates that multiple pumps will be needed if the maximum output is 7 kW, requiring at least 5 pumps. If 5 pumps were being used at 200 W, the total power draw is about 1 kW. This is still significantly less power consumption than the compressor but increases the initial cost of the system. However, from the results presented there are opportunities for increasing the heat output. These include increasing the temperature difference, lowering the mass charge of the system to allow for higher temperature at equivalent pressures, and running the VFD at frequencies greater than 60 Hz.

During the course of the experiments the pressure of the system was a concern. The system was pressure rated to 9.75 MPa and at the time it was not well understood which temperature in the system would dictate the pressure. Understanding the process from subcritical to supercritical and how the cycle executes along with experimental results shows that the system pressure is mainly dependent on the pump inlet temperature. Figure 7 shows the relationship between the system pressure and pump inlet temperature. This indicates that as long as the CO<sub>2</sub> can be sufficiently cooled by the cooling HX, the pressure of the system can be kept at safe operating conditions while increasing the temperature of CO<sub>2</sub> leaving the heating heat exchanger. The result would be a larger temperature difference, leading to an increased heat output. The current setup can be used to test this but is limited by the temperature output of the hot water loop and the HXs. Assuming that the maximum temperature leaving the heating HX is 336 K, and the loop is able to cool this CO<sub>2</sub> to 319 K, just below the maximum pressure condition, the temperature difference is 17 K. If this is done at 60 Hz, the mass flow rate is about 0.12 kg/s. From the fit in Figure 6 the heat output is about 17 kW, more than doubling the heat output that was measured in the experiments, reducing the number of pumps.

Another possible option is to decrease the amount of CO<sub>2</sub> in the system. If the mass present in the system is decreased, the CO<sub>2</sub> could be heated to a higher temperature at the same pressure. This would become an optimization problem in itself because the specific heat also decreases with temperature; what mass charge gives the maximum heat output over the range of temperatures considered? This is not fully understood so an estimate of the benefit cannot be made.

The final opportunity considered for improvement is running the VFD at frequencies greater than 60 Hz. If

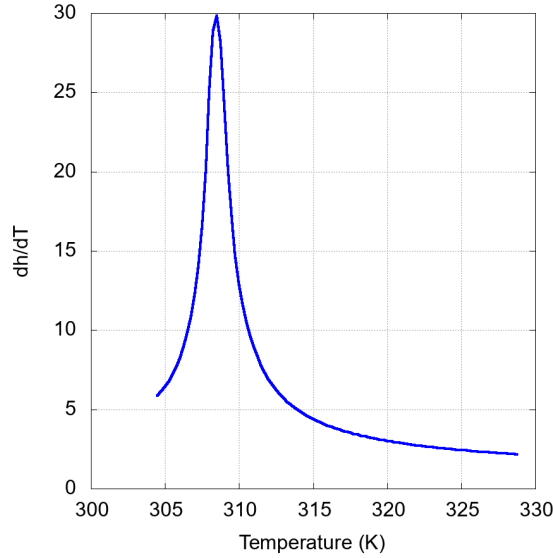


Figure 8: The sensitivity of enthalpy with temperature explains why such large uncertainty is associated with the heat transfer calculations.

the effect of density changes is assumed negligible (reasonable assumption by Figure 5, a) a linear fit between the mass flow rate and the VFD frequency can be made (Figure 5, b),

$$\dot{m} = 0.002f_{VFD} + 0.001. \quad (15)$$

If the VFD is operated at 75 Hz, the mass flow rate is expected to be 0.151 kg/s, according to Eqn. 15. If this mass flow rate is performed for the same temperature differences, the performance can be estimated by the fit given in Figure 6, and this estimate is given in the figure shown by the black wireframe squares. An increase in maximum output of 1.5 kW is estimated which is about a 13% increase from 60 Hz. If the pump is operated at 75 Hz *and* the temperature difference is increased to the previously stated 17 K, the heat output is estimated at 20.5 kW. The required number of pumps is now 2 for our purposes with this increased performance.

Finally, some of the challenges encountered in this work are acknowledged, in particular, problems that were faced with the CO<sub>2</sub> pump and with the uncertainty in the measurement are discussed.

The CO<sub>2</sub> pump was designed for liquid circulation but modified by the manufacturer to endure the higher working pressure of supercritical CO<sub>2</sub>. Unfortunately, the initial design did not consider the aspect of a gas-like fluid being present in the pump and potentially being trapped in any of the internal components. When the system was operated and then vented, gas was trapped in a sleeve in the impeller, which expanded and plastically deformed when the system was vented. The solution was to provide vents on the components that can potentially trap gas.

The final consideration that should be mentioned are the large error bars on the heat calculations (Figure 6). Performing an uncertainty analysis on the measurements it was a surprise that the uncertainty was so large (about 1.5 kW) on the measurements given that calibrated thermocouples were used. Figure 8 gives insight into how slight uncertainty in temperature measurements can lead to large uncertainties in the heat transfer calculations (Eqns. 2 and 3). A number of the experiments were performed between 308 and 313 K where small changes in temperature can lead to large change in enthalpy and thereby increases the uncertainty in the heat transfer calculations. This should have been expected considering the known instability of the specific heat in this temperature and pressure range.

## 6. Conclusion

This work showed that given an appropriately designed CO<sub>2</sub> pump, supercritical CO<sub>2</sub> can be circulated effectively with a centrifugal pump. The work presented on the ability of the pump and supercritical CO<sub>2</sub> to be used as a secondary loop between a heat source (ASHP) and heat sink (indoor AHU) in a test loop setup. While the amount of heat that was transferred between the source and the sink was somewhat below the requirement for the full scale ASHP, the testing gives indications of how many pumps would be needed if the heat transfer loop was operated as is. More importantly the research showed that there exist opportunities for improvement which included increasing the temperature difference while maintaining system pressure, increasing the VFD frequency, and adjusting the system mass charge. The two former points of improvement could be estimated with the work done and showed that there is a potential to more than double the capacity of the output by appropriate changes in operating conditions. Further work should focus on investigating the concept of optimal charge for pumped supercritical CO<sub>2</sub> systems.

## Acknowledgements

The authors would like to acknowledge the California Energy Commission, San Diego Gas and Electric, and Southern California Edison for funding this research under EPC-19-014.

## References

- [1] Environmental Protection Agency, *Final Rule – Phasedown of Hydrofluorocarbons: Establishing the Allowance Allocation and Trading Program under the American Innovation and Manufacturing (AIM) Act*, 2021.
- [2] Electric Power Research Institute, "Environmentally Friendly Advanced Refrigerant Options in Commercial HVAC Applications," Electric Power Research Institute, Palo Alto, 2022.
- [3] J. M. Cubas, H. Stel, M. Neto, L. Da Silva, G. Romero and R. Morales, *Numerical Simulation of the Flow of Supercritical CO<sub>2</sub> in a Multistage Centrifugal Pump*, Rio de Janeiro, Brazil: SPE Brazil Flow Assurance Technology Congress, 2022.
- [4] S. Kim, J. Lee, Y. Ahn, J. Lee, Y. Addad and B. Ko, "CFD Investigation of a Centrifugal Compressor Derived from Pump Technology for Supercritical Carbon Dioxide as a Working Fluid," *The Journal of Supercritical Fluids*, vol. 86, pp. 160-171, 2014.
- [5] L. Bergamini, "Centrifugal Pumps For Co<sub>2</sub> Applications," in *Twenty-Seventh International Pump User Symposium*, Houston, TX, 2011.
- [6] E. W. Lemmon, I. H. Bell, M. L. Huber and M. O. McLinden, *NIST Standard Reference Database 23: Reference Fluid Thermodynamic and Transport Properties-REFPROP, Version 10.0*, National Institute of Standards and Technology, 2018.
- [7] R. a. W. W. Span, "A New Equation of State for Carbon Dioxide Covering the Fluid Region from the Triple-Point Temperature to 1100 K at Pressures up to 800 MPa," *J. Phys. Chem. Ref. Data*, vol. 25, no. 6, pp. 1509-1596, 1996.
- [8] J. Taylor, *Introduction to Error Analysis, the Study of Uncertainties in Physical Measurements*, 1997.
- [9] A. J. Wheeler and A. R. Ganji, *Introduction to Engineering Experimentation*, Saddle River: Pearson, 2010.